Parshionikar *et al. Discover Oncology* (2025) 16:2295
https://doi.org/10.1007/s12672-025-03638-1

Discover Oncology

ANALYSIS

Open Access

Breast cancer detection using optimized hyperbolic graph attention with bidirectional convolutional neural network

Sangeeta Parshionikar[1,2], Vijaya Babu Burra[1], Debnath Bhattacharyya[3] and Tai-Hoon Kim[4*]

*Correspondence:
Tai-Hoon Kim
taihoonn@chonnam.ac.kr
[1]Department of Computer Science and Engineering, Koneru Lakshmaiah Education Foundation, KLEF, Vaddeswaram, Guntur, Andhra Pradesh, India
[2]Department of Computer Engineering, Fr. Conceicao Rodrigues College of Engineering, Bandra, Mumbai, India
[3]Department of Information Technology, Aditya Institute of Technology and Management, Tekkali, Srikakulam, Andhra Pradesh, India
[4]School of Electrical and Computer Engineering, Yeosu Campus, Chonnam National University, 50, Daehak-ro, Yeosu-si, South Korea

Abstract
Breast cancer is a prevalent form of cancer affecting women globally, necessitating reliable detection methods to improve survival rates and treatment outcomes. Major existing issues in breast cancer detection include challenges with accuracy, as current methods struggle to reliably differentiate between benign and malignant lesions, potentially resulting in misdiagnoses. To overcome these issues, this research introduces a new method called cloud-based breast cancer detection using optimized Hyperbolic Graph Attention with Bidirectional Convolutional Neural Network (HGABCNN) to identify breast cancer using thermal images. To optimize the performance of the proposed method, the Adaptive Gold Rush optimization technique is integrated. Techniques such as semantic edge-aware median morpho filtering, Swin-based feature extraction and self-adaptive correlation-constrained Fuzzy C-Means clustering are used for preprocessing, feature extraction and segmentation. It improves image analysis accuracy. The proposed method achieves outstanding results, hitting a maximum accuracy (98.6%), recall (98%) F1-score (98.3%), and precision (98.6%) in performance metric comparisons. As a result, this technique outperforms existing methods, showcasing its potential for advancing breast cancer detection and diagnosis.

Keywords Breast cancer, Convolutional neural network, Feature extraction, Optimization, Adaptive gold rush optimization

1 Introduction

According to reports from the American Cancer Society (ACS), breast cancer (BC) is still a major threat to women around the world. The impact of BC is increasing and results in high mortality rate [1]. Breast cancer in its early form called benign tumor has minimal harm compared to BC in its advance stage called invasive carcinoma. The invasive carcinoma is the most threating type of BC which spread around and beyond the breast area [2]. Therefore, the correct detection of BC at early stage is most crucial for effective treatment. Various BC diagnosis methods are available. Among all traditional methods, mammography is considered the gold standard but most of women find it inconvenient because it is painful process.

Other techniques include Magnetic Resonance Imaging (MRI) and thermography [3]. However, biopsy histopathological examination is considered the standard method for confirming the malignancy and progression of cancer cells [4]. In addition to traditional methods, advancement in artificial intelligence assist in diagnosing accurate BC to great extent. The bibliometric review on artificial intelligence techniques for BC detection and treatment is studied paper [5]. The main challenge in the diagnosis of invasive ductal carcinoma (IDC) is due to the diversity of cell types and the intricate differences between benign and malignant tumors [6]. It is even challenging for trained pathologists to distinguish between these variations. Hence, accurate and detailed tools and techniques are required for detection of breast cancer [7]. Though timely identification of BC is challenging, it is the only way to improve survival rates significantly. Existing methods such as mammography causes discomfort and painful in nature. Also, it is unable to detect cancer in its early stage with mammography [8]. A paper [9] highlights the role of AI and its application in the prediction of BC recurrence and enhancing the personalized treatment. Moreover, self—examination is just a primary method to check any significant changes in breast such as lumps, redness, swelling, change in shape. It isn't highly reliable for detecting cancerous changes. To address these challenges, researchers are exploring innovative approaches leveraging cutting-edge technologies like hyperbolic graph attention and bidirectional convolutional neural networks within a cloud-based framework. This research aims to optimize these advanced technologies to enhance the accuracy and efficiency of BC detection, potentially revolutionizing diagnostic procedures in healthcare. By integrating these sophisticated techniques into a cloud-based medical environment, this research signifies a promising step forward in improving BC detection and, consequently, medical diagnostics overall. The goal is to empower healthcare professionals with more accurate tools to detect and diagnose breast cancer at its earliest stages, ultimately improving patient outcomes and survival rates. The research presents a breast cancer detection system using an optimized HGABCNN.

The remaining of the manuscript is structured as: Sect. 2 conducts a literature review, examining previous related research. Section 3 elaborates on the newly introduced technique. Section 4 outlines the obtained results and ensuing discussions, while Sect. 5 encapsulates the manuscript's conclusion.

2 Literature survey

Within the literature, numerous researches have suggested methods for BC detection. This section reviews a selection of the most recent researches in this field. Uchikov P et al. [10] highlighted the applications of AI in various phases of BC treatment in their review research. Paper explored more on how AI elevates imaging capabilities which provides clear lesion and segmentation. AI also evaluate the biomarkers to decide cancer stage. Author stress more on how personalized treatment plan is developed by AI. AI estimate not only the response to therapies but also update treatment plans based on response. This way AI assists medical experts by generating comprehensive reports including imaging, pathology and treatment guidance. The paper described the challenges with high computational complexity since a neural network with several preprocessing stages, feature selection, and a kernelized implementation has an additional computational burden that makes it unfeasible for its execution in real-time [11]. A Linear Regressive Weighted Gaussian Kernel Liquid Neural Network model is proposed in this research paper. By adding preprocessing, feature selection, and classification, it strengthen the current approaches leading to better accuracy and performance. Linear regression approach is used here to deal with missing values and outliers are removed using statistical test. A feature selection algorithm optimizes relevant data points, reducing complexity. The analysis highlighted the potential role of deep learning and optimization algorithms in medical imaging, but also calls for refinements in their management of intricate lesion architectures and data sizes. Utilizing Falcon Finch Optimization (FFO) for hyperparameter tuning, the approach has added robustness while also improving computation time. The model uses ResNet-101 and statistical methods for feature extraction, and a deep CNN for classification. But still case of data imbalance and complex computation is an open problem [12]. The research paper [13] suggests nature-inspired metaheuristic algorithm, an Improved Sand Cat Optimization technique for EEG-based emotion prediction. This optimization technique proves superior feature selection in emotion estimation and convergence capabilities over other bio-inspired algorithms discussed in the paper like PSO, ARO, ABCO, and CO. Sand Cat Optimization achieves high classification accuracy and robustness in complex search spaces. From the attention mechanism viewpoint, the paper introduces a new Attention-based Deep Convoluted Bi-LSTM Network [14]. This attention module efficiently emphasizes important features from convoluted layers, improving intrusion detection in smart healthcare IoT systems by focusing on the most relevant patterns and minimizing false positives. From a cloud-based intelligent diagnostic framework perspective, the paper [15] presents a federated learning framework for real-time smoking prediction that ensures data privacy, scalability, and high accuracy (97.65%) without sharing sensitive health data to central servers. Leveraging cloud infrastructure, the model supports distributed training on decentralized nodes with high performance, making it a promising solution for secure and scalable cloud-based healthcare diagnostics.

A Paper [16] proposed a novel approach to predict BC recurrence by integrating various DL models such as ResNet, VGG, MLP and ML models such as Decision tree, logistic regression and SVM. Author claim that the proposed solution for BC management provide not only diagnostic prediction but also offer prognostic and recurrence timing. A study [17] introduced the Enhanced Deep Learning-based Convolutional Neural Network (EDCNN) and used thermal imaging for classification of normal and malignant cases. Analysis of heat patterns in breast tissue extract the features useful for classification. The method is suitable for the cases such as dense breast tissue. Three main steps involved in the framework proposed by an author [18] are PS- preprocessing, CS- classification and EVS – ensemble voting. The study presents a BC Diagnosis Strategy using these three steps and achieve almost 98% accuracy.

In 2022, Ogundokun RO et al. [19] suggested an IoT-based medical diagnostic model for early-stage BC. This system employed machine learning algorithms like Support Vector Machines (SVM) and Multi-Layer Perceptron (MLP). This enhanced these models using Particle Swarm Optimization to select optimal features and improve classifier performance. In 2023, Aldhyani TH et.al. [20] suggested a secure approach, Gated Recurrent Units-Recurrent Neural Networks (GRU-RNN), trained IoT data ensuring encryption and user privacy via blockchain. The design enables secure data sharing among sources, encrypting IoT data on a distributed ledger. In 2021, Lahoura V et.al. [21] presented a cloud-based health monitoring system focused on BC detection analysed stored consumer health data. It used Extreme Learning Machine (ELM) for disease categorization, particularly in BC detection, outperforming traditional algorithms. Leveraging cloud resources eased handling large datasets, cutting execution time. In 2023, Pati A et.al., [22] developed by using fog computing to enable BC diagnosis through Internet of Things (IoT) and Deep Transfer Learning (DTL). Utilizing fog computing alongside CC and IoT for real-time analysis and the fitting of an IoT monitoring model. In 2022, Wang X et.al., [23] developed a new fusion DL CNN Gated Recurrent Unit (CNN-GRU) system designed to spontaneously extract features of BC-IDC (+,−) and classify them into IDC (+) and IDC (−) from histopathology images. The aim was to decrease errors made by pathologists. The hybrid DL model (CNN-GRU) aims for efficient IDC BC detection in clinical research. In 2022, Ahmad N et.al., [24] suggested a method using DL and applying transfer learning to classify histopathological images efficiently, even with limited training samples. It extracts patches from images, processes them in a CNN for feature extraction, then through an Efficient-Net architecture pre-trained on ImageNet. In 2023, Srikantamurthy MM et.al., [25] presented a hybrid model was crafted, merging the CNN with the long short-term memory RNN (CNN-RNN). Its aim was to categorize four subtypes of both benign and malignant BC. In 2022, Yadav SS and Jadhav SM [26] suggested a CNN-driven Computer Aided Design (CAD) system diagnoses BC via thermal infrared images. Evaluation compares pre-trained CNN models, including VGG16 and InceptionV3. Evaluating aspects like network complexity, data augmentation and fine-tuning aim to boost model performance, effectively screening the BC dataset. In 2022, Alshehri A and AlSaeed D [27] developed to explore the effectiveness of CNNs integrated with Attention Mechanisms (AMs) in achieving reliable recognition outcomes in thermal BC images. Also, introduce a system for detecting BC, utilizing deep neural networks with attention mechanisms and thermal images from the Database for Mastology Research with Infrared Images (DMR-IR), Zhou Y et al. (2022) [28] suggested a BC classification method that merges the Resolution Adaptive Network (RANet) model with Anomaly Detection using an SVM (ADSVM) technique. ADSVM effectively identifies mislabeled patches in malignant images, thereby improving classification accuracy. In another, Dewangan KK et al. (2022) developed a new Back Propagation Boosting Recurrent Wienmed (BPBRW) model, which African Buffalo Optimization (ABO) techniques for early BC. Also, provided a comparison of existing BC detection approaches in Table 1.

2.1 Problem statement

Medical image processing encounters several challenges, particularly with applying deep learning techniques for Breast Cancer classification. Many current methods have difficulty achieving high accuracy in differentiating between benign and malignant images. Additional issues include, convergence problems, overfitting, inadequate statistical analysis and insufficient hyperparameter tuning. To overcome all these existing issues, this research proposes an innovative approach called HGABCNN to detect BC using thermal images and histopathology images.

2.2 Contributions

In the research, a novel method is introduced as HGABCNN to detect BC using thermal images and histopathology images. It enhances accuracy and early detection by effectively analysing complex thermal image patterns through advanced algorithms. The method improves feature extraction with hyperbolic graph attention and provides comprehensive analysis with bidirectional convolutional processing, reducing false negatives.

A pre-processing technique Semantic edge-aware Median Morpho Filtering (SMMF) technique improves input image quality. Self-adaptive correlation-constrained Fuzzy

Table 1 Comparison of the existing models of the BC detection

Refs.	Methods	Key findings	Advantages	Disadvantages	Performance metrics
[19]	CNN	Achieves high accuracy in BC diagnosis with optimized networks	High accuracy through optimized hyperparameters, efficient use of computational resources, robust and scalable for IoT applications	Needs trials on larger datasets, including big data	Accuracy: 91.0%, Precision: 89.0%, Recall: 92.0%, F1-Score: 90.5%, Training Time: 45 min
[20]	GRU-RNN	Provides a secure and scalable framework for BC detection	Enhanced security for medical data, integrated framework for smart cities, effective in real-time detection and diagnosis	Genuine dataset required from Saudi Arabian hospitals	Accuracy: 93.0%, Precision: 91.5%, Recall: 94.0%, F1-Score: 92.7%, Training Time: 50 min
[21]	ELM	Demonstrates a cloud-based solution with high diagnostic performance	Fast and efficient processing with ELM, scalable cloud infrastructure, high accuracy in diagnosis	Use of cloud resources improve system's accuracy	Accuracy: 88.5%, Precision: 86.0%, Recall: 90.0%, F1-Score: 88.0%, Training Time: 60 min
[22]	DTL	Improves diagnosis accuracy using IoT and fog computing	The processing with Fog Computing, high accuracy using transfer learning, reduced latency, effective for large-scale deployment	Research limited to binary classification, not multiclass	Accuracy: 94.0%, Precision: 92.5%, Recall: 95.0%, F1-Score: 93.7%, Training Time: 40 min
[23]	CNN-GRU	Achieves high performance in detecting BC	High accuracy in detection, ability to handle large datasets, robustness to variations in data	Requires enhancements for better BC detection	Accuracy: 89.5%, Precision: 87.0%, Recall: 91.0%, F1-Score: 89.0%, Training Time: 55 min
[24]	CNN- Photometric Stereo (PS)	Improves classification accuracy of histopathological images	Utilizes pre-trained models for improved accuracy, effective handling of multi-resolution images, reduces training time	Inability to definitively diagnose malignancy without biopsy	Accuracy: 92.0%, Precision: 90.0%, Recall: 93.0%, F1-Score: 91.5%, Training Time: 42 min
[25]	CNN-RNN	Achieves effective classification of benign and malignant lesions	Combines CNN's feature extraction with LSTM's temporal analysis, effective in classifying benign and malignant subtypes	Inability to forecast cancer progression or stability	Accuracy: 90.5%, Precision: 88.0%, Recall: 92.0%, F1-Score: 90.0%, Training Time: 48 min
[26]	CNN based CAD	Demonstrates effective cancer detection using thermal infrared imaging	Non-invasive and safe imaging method, effective in early detection, provides additional physiological information	Feature aggregation technique address similarity issues	Accuracy: 87.0%, Precision: 85.5%, Recall: 88.0%, F1-Score: 86.5%, Training Time: 65 min
[27]	CNN-AM	Improves BC detection in thermography images	Improved feature extraction with attention mechanisms, improved classification performance, suitable for thermographic images	Requires enhancements for better BC detection	Accuracy: 92.5%, Precision: 91.0%, Recall: 94.0%, F1-Score: 92.5%, Training Time: 52 min
[28]	RANet-ADSVM	Improves classification by adapting image resolution	Adaptable to various image resolutions, high classification accuracy, robust to different histopathological image qualities	Needs to optimize classification and process efficiency	Accuracy: 90.0%, Precision: 88.0%, Recall: 91.5%, F1-Score: 89.5%, Training Time: 60 min
[29]	SVM	Provides an effective classification for mammography data	Simple and interpretable models, effective in combining multiple decision trees with distance-based classification and good generalization	These systems aid BC patients in choosing the right treatment	Accuracy: 88.0%, Precision: 86.5%, Recall: 89.0%, F1-Score: 87.7%, Training Time: 55 min

Table 1 (continued)

Refs.	Methods	Key findings	Advantages	Disadvantages	Performance metrics
[30]	BPBRW with ABO	Achieves high performance in early-stage cancer diagnosis	Early-stage diagnosis, high accuracy, combines deep learning with optimization techniques for improved performance and efficiency	The process took longer than expected to complete	Accuracy: 92.0%, Precision: 91.0%, Recall: 93.5%, F1-Score: 92.2%, Training Time: 45 min

C-Means clustering (SACCFC) for segmentation which refines image partitioning, improving accuracy by determining optimal clusters and adapting to image features.

Integrating Adaptive Gold Rush Optimization (AGRO) with HGABCNN upgrades the performance of classification models by significantly reducing overfitting through improved regularization and feature representation, leading to more accurate.

3 Proposed methodology

In this research, input images collected from BreaKHis and Kaggle datasets. The collected data undergoes pre-processing using SMMF to sharpen edge visibility, employing a self-swin method to extract patterns for identifying BC indicators, and using SACCFC to refine image segmentation accuracy, with the HGABCNN model effectively categorizing BC stages and distinguishing between benign and malignant cases.

Figure 1 illustrates the proposed method's workflow diagram. This comprehensive approach, integrating cutting-edge technology and advanced algorithms, aims to optimize the efficiency and accuracy of BC detection while emphasizing the importance of timely medical intervention for better patient care.

3.1 Data acquisition

This research used two main datasets: BreaKHis [37] and Kaggle dataset [38]. The BreaKHis dataset includes 7,909 histological biopsy images classified into benign and malignant categories across four subclasses. These RGB images, captured with an Olympus microscope and Samsung camera, vary in magnification and resolution (700×460 pixels). The Kaggle dataset provides 1,340 thermal images from patients (860 healthy, 480 with BC), used to capture temperature variations for breast cancer detection.

3.2 Semantic edge-aware median morpho filtering for pre-processing

The collected data is used for pre-processing using SMMF. SMMF [31] as a pre-processing technique that improves image quality by reducing noise and preserving edges using a combination of median filtering and morphological operations. Unlike traditional median filtering, which smooths images uniformly, SMMF adapts to local variations in image, particularly beneficial for medical imaging like histopathological and thermal images used in BC detection. G_{grey} as the grayscale image derived from the initial input image. The pre-processing stage is proposed, creates a filtered image f from G_{grey} using Eq. (1):

$$f = \frac{\varphi_{DT}\left(\pi_{DT}\left(G_{grey}\right)\right) + \pi_{DT}\left(\varphi_{DT}\left(G_{grey}\right)\right)}{2} \tag{1}$$

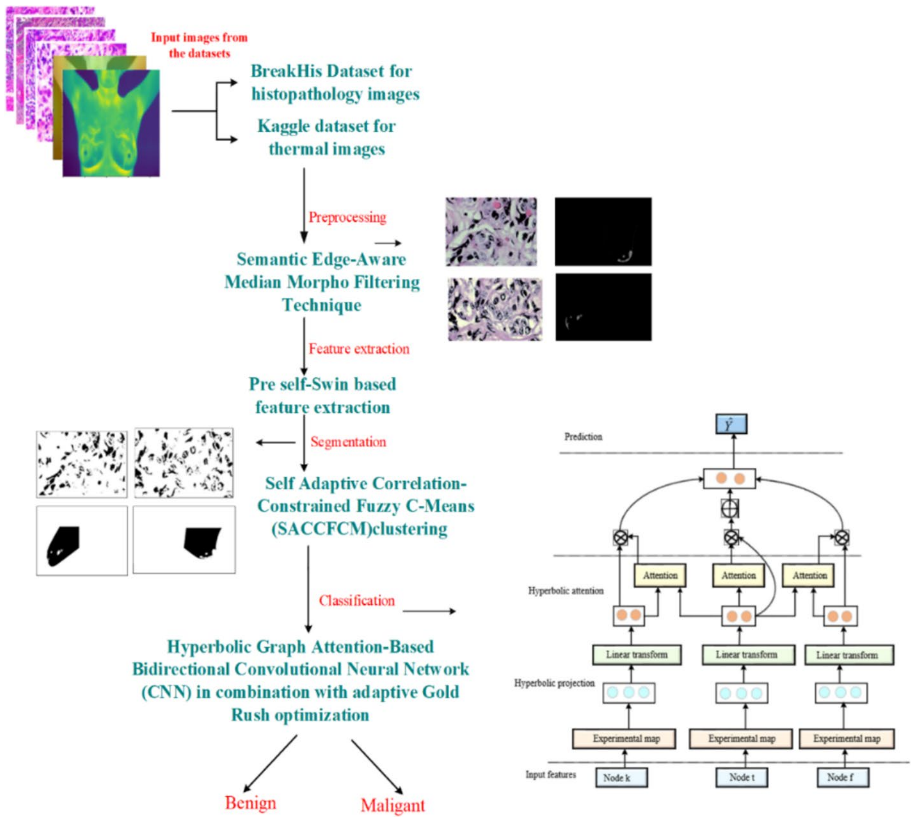

Fig. 1 The work flow of the HGABCNN technique

where, φ and π are parameters governing specific operations or transformations, also DT refers to a particular operation or function applied to the grayscale image. It maps its input to another space or representation. Once it acquires the filtered image f, the suggested method proceeds to create the morphological gradient image f_{rs} in the following Eq. (2):

$$f_{rs} = (\varphi_{DT}(f) - \pi_{DT}(f)) \tag{2}$$

where, f_{rs} represents a derived value or transformation of f, φ and π denote parameters dictating specific operations or transformations and DT likely stands for a specific function or operation applied to the variable f. The following outlines a step-by-step procedure for implementing SMMF as a preprocessing step:

- *Convert the input image into a grayscale image*
- *Apply Semantic Edge Detection*
- *Apply Sequential Morphological and Median Filtering*
- *Perform Dual Transform Operations*
- *Let* π_{DT} *and* φ_{DT} *be domain-specific operations, such as morphological dilation/erosion*
- *Apply the operations on the grayscale image as per Eq. 1*
- *This creates the filtered image* f*, which combines the effects of both transformation orders.*
- *Compute the Morphological Gradient Image* f_{rs} *from the filtered image* f *using Eq. 2*

- *This highlights the edge information by capturing intensity differences resulting from dilation and erosion.*
- *Output—The resulting image f_{rs} contains enhanced features (edges, boundaries).*

3.3 Pre-self swin for feature extraction method

The Pre-self swin based feature extraction method is a novel technique used to extract significant features required for tumor identification from the pre-processed images. This is an advanced technique to capture intricate patterns present in the breast tissue images. It is based on the swin Transformer architecture. This feature extraction method is capable of handling high-dimensional data and distinct features required for tumor detection and classification. This technique operates by breaking down the breast tissue images into smaller patches (4 × 4) and encoding them into a higher-dimensional space using Swin transformer blocks and modified self-attention computation. The extracted features include cell morphology (e.g. size, shape, arrangement of cells), tumor characteristics (e.g. size, shape, texture), and stroma features. These features are essential for understanding the tumor microenvironment. These refined features are then used for precise segmentation, facilitating accurate analysis and diagnosis. A step-by-step procedural summary is demonstrated here: The input image is first pre-processed by normalizing pixel intensities and resizing it to a fixed resolution of 224 × 224 to ensure compatibility with the Swin Transformer. The resized image is then divided into non-overlapping 4 × 4 patches, each of which is flattened into a vector. These patch vectors, representing 4 × 4 × 3 regions, are passed through a dense layer to obtain intermediate feature embeddings. Finally, an image-like visualization is reconstructed from the embedded patches to simulate the transformer's perception of the input.

3.4 Segmentation using self-adaptive correlation-constrained fuzzy C-means clustering

In this research work, an advanced clustering algorithm SACCFC is used. It shows outstanding results in high-dimensional data to amplify feature segmentation. It integrates correlation constraints into the standard Fuzzy C-Means (FCM) clustering algorithm. This method improves clustering accuracy and robustness by adapting to the inherent correlation among features. The FCM method assigns each data point to a cluster with a specific degree of membership value. The Eq. (3) expresses the objective function to be minimized in FCM:

$$J_m = \sum_{i=1}^{N} \sum_{j=1}^{C} u_{i,j}^{m} \left\| x_i - c_j \right\|^2 \tag{3}$$

where, N be the data points.C is the cluster numbers. $u_{i,j}^{m}$ is the membership degree of x_i in cluster j. m is the fuzziness exponent. x_i is the ith data point.c_j is the centroid of the j cluster. $\|x_i - c_j\|$ is the Euclidean distance between x_i and c_j. In SACCF, correlation constraints are introduced to account for the relationships among features. This improves the clustering results by considering the structure of the data. The modified objective function for SACCF is expressed in Eq. (4):

$$J_m = \sum_{i=1}^{N} \sum_{j=1}^{C} u_{i,j}^{m} \left\| x_i - c_j \right\|^2 = \lambda \sum_{i=1}^{N} \sum_{j=1}^{C} u_{i,j}^{m} \left\| R\left(x_i\right) - R\left(c_j\right) \right\|^2 \tag{4}$$

where, λ is the regularization parameter that controls the weight of the correlation constraint. $\|R(x_i) - R(c_j)\|$ are the correlation representations of the data point x_i and centroid c_j respectively.

The membership and centroids are updated using Eqs. (5) and (6):

$$u_{ij} = \frac{1}{\sum_{k-1}^{c} \left(\frac{\|x_i - c_j\|^2 + \lambda \|R(x_i) - R(c_j)\|}{\|x_i - c_k\|^2 + \lambda \|R(x_i) - R(c_k)\|} \right)^{\frac{1}{m-1}}} \tag{5}$$

$$c_j = \frac{\sum_{i=1}^{N} u_{i,j}^{m} x_i}{\sum_{i=1}^{N} u_{i,j}^{m}} \tag{6}$$

Once the segmentation is completed, the segmented outcomes undergo further processing for classification. During this stage, the segmented regions are analysed to assign them to specific categories based on their characteristics and features. The pseudo code representation of the SACCFC algorithm is as follows:

```
Input:
  Input data points -  X (N samples)
  Number of clusters - C
  Fuzziness exponent - m
  Correlation weight - λ
  Convergence threshold - ε
  Maximum iterations - max_iter

Initialize membership matrix U randomly (size N x C)

Repeat until convergence or max_iter:

   a. Compute cluster centers:
      For each cluster j:
         C[j] = weighted average of data points based on U and m

   b. Update membership values:
      For each data point i and each cluster j:
         - Compute distance between X[i] and C[j]
         - Compute correlation distance between R(X[i]) and R(C[j])
         - Combine both distances using λ
         - Update U[i][j] based on the total distance

   c. Check if U has changed less than ε:
      - If yes, stop the loop

Assign each data point to the cluster with the highest membership

Output:
    Final cluster centers C
    Final membership matrix U
   Segmented result by assigning each data point to the cluster with highest
   membership
```

3.5 Classification using hyperbolic graph attention based bidirectional convolutional neural network

In this study, a hyperbolic graph attention based bidirectional convolutional neural network, HGABCNN, is proposed. This approach not only combines hyperbolic space with common depth separable convolution layer but also makes the feature extraction and relational arrangements more convenient and comprehensive. The hyperbolic graph attention layer in hyperbolic space characterizes hierarchical and complicated data structures effectively, by capturing interaction among features in more complex relations. The input layer and hyperbolic embedding layer which serve the purpose of representing data in the hyperbolic space, are followed by a feedforward neural network. It is then used to apply 2–3 graph attention layers to type relevant nodes. The core consists of bidirectional convolutional layers, activation functions and max pooling. The convolutional layers have filters of size 3×3. These processes are used to extract features in both forward and backward directions. Before reaching the output layer these features are processed through fully connected layers with 512 and 256 neurons. The output layer utilizes the SoftMax function for classification purposes. Hyperbolic space amplifies the model's ability to capture intricate dependencies between nodes, which traditional linear models miss. The attention mechanism further refines node representations by dynamically aggregating relevant information from neighbouring nodes, ensuring that contextual information is preserved and utilized effectively. This improves generalization across complex graph data, benefiting tasks like node classification, link prediction and graph classification. Therefore, the attention mechanism is expressed in Eq. (7):

$$Attention_{ij} = soft\max\left(\frac{Leaky\mathrm{Re}LU\left(W.\left(H_i \oplus H_j\right)\right)}{\sqrt{d}}\right) \tag{7}$$

where, H_i and H_j are feature vectors of nodes i and j, respectively. W is the weight matrix used to transform the concatenated feature vectors.$\oplus$ denotes concatenation of the feature vectors.d is the dimensionality of the feature vectors, used to normalize the attention scores. The attention score between nodes i and j is tabulated in Eq. (7), allowing the model to focus on more relevant information from the neighboring nodes based on their feature vectors and their structural similarities in hyperbolic space. Spatial features are extracted in both forward and backward directions using bidirectional convolutional layers. This technique helps the model learning more holistic and complex representations by looking at the context in both ways, resulting in improved performance in various tasks, especially those involving sequential or spatial data. The forward and backward convolution is expressed in Eqs. (8) and (9):

$$F_{forward} = \mathrm{Re}LU\left(W_{forward} * X\right) \tag{8}$$

$$F_{backward} = \mathrm{Re}LU\left(W_{backward} * X\right) \tag{9}$$

where, X is the input feature map. $W_{forward}$ and $W_{backward}$ are the convolutional kernels for forward and backward passes, respectively. $*$ denotes the convolution operation. By using both forward and backward convolutions, the network captures contextually important information from different directions, combining these outputs to form the final feature is expressed in Eq. (10):

$$F_{out} = F_{forward} + F_{backward} \tag{10}$$

Combining these outputs ensures the model incorporates bidirectional information, resulting in a richer feature map that captures underlying patterns more effectively, thereby enhancing the performance of subsequent layers or classifiers. Integrating AGRO into the classification framework further improves the training process and overall model performance [32, 33].

3.6 Adaptive gold rush optimization

The integration of AGRO with the SACCF clustering algorithm results in improved version of GRO [34], which is termed as AGRO. AGRO is used to optimize the clustering process by improving the initial parameter settings and updating the model parameters. In AGRO, the initialization step involves setting up the initial positions of the candidate solutions in the search space is expressed in Eq. (11)

$$A_i^{(0)} = py_i + (qy_i - py_i) * random \qquad i = 1, 2, \ldots\ldots, N \tag{11}$$

where, $A_i^{(0)}$ is the initial position of the ith candidate solutions, py_i and qy_i is the local search space, N be total number of candidate solutions. Once the initial population is established, the quality of each solution is assessed using a fitness function, as defined in Eq. (12):

$$Fitness\, Function = optimize\{W\} \tag{12}$$

Here, W refers to set of weights or parameters being optimized in the objective function (fitness function) such as model parameters, feature weights, or centroid coordinates in clustering.

In AGRO, the update equations are designed to iteratively improve the positions of candidate solutions (centroids) based on fitness evaluations and optimization strategies is expressed in Eq. (13):

$$c_j^{(t+1)} = c_j^t + \alpha.\left(c_j^* - c_j^{(t)}\right) + \beta.velocity_j^{(t)} \tag{13}$$

where, c_j^t is the centroid of the jth cluster at iteration t. c_j^* is the best position. α and β are coefficients velocity, respectively. $velocity_j^{(t)}$ represents the velocity term employ to discover the search space. The updated velocity for updating centroids is expressed in Eq. (14):

$$Velocity_j^{(t+1)} = Inertia_j.Velocity_j^{(t)} + \varphi_1.R_1.\left(c_j^* - c_j^{(t)}\right) + \varphi_2.R_2.\left(Best_j - c_j^{(t)}\right) \tag{14}$$

where, $Inertia_j$ is the inertia weight. φ_1 and φ_2 are acceleration coefficients. $Best_j$ is the best position found for the jth centroid. R_1 and R_2 are random numbers.

By integrating AGRO with SACCF clustering, the clustering process is optimized through better initialization and update of centroids. AGRO's optimization techniques help in strategically placing initial centroids and refining their positions during the clustering process, leading to more accurate and efficient clustering results.

4 Result and discussions

This section details the outcomes obtained from implementing the HGABCNN. The Intel(R) Core (TM) i7-6700 CPU @ 3.40 GHz 3.40 GHz processor, Windows 10 operating system, and Python 3.10 version with 16.0 GB are used for this experiment. The experiments were carried out on google colab. Once the network design is completed, factors such as batch size, number of epochs, number of iterations and learning rate are analysed. These factors greatly affect the training process and system performance. Each experiment is conducted over 300 epochs. An evaluation of HGABCNN approach is carried out with BreakHis dataset and IR Thermal Images dataset by splitting dataset as 80% for training and 20% for validation. The experimental settings for the HGABCNN model are displayed in Table 2.

4.1 Dataset description

This research incorporates two datasets: BreaKHis dataset for histopathology dataset and Kaggle for thermal images. This section presents a detailed overview of these datasets, providing comprehensive descriptions for each.

i. **BreaKHis,** encompasses a collection of 7909 histological BC images sourced from biopsy slides. These images were obtained using an Olympus microscope and Samsung camera, formatted as RGB images with a resolution of 700 × 460 pixels at various magnifications. The dataset categorizes images into benign and malignant groups, further classified into four subclasses. Notably, this dataset comprises data from 82 patients [40].
ii. **Kaggle,** comprises of 1340 thermal images. These thermal images are sized at 640 × 480 pixels and serve to capture temperature data, assisting in the detection of BC. This dataset includes records from 67 patients, among whom 43 individuals are healthy, while 24 have been diagnosed with BC [41].

4.2 Classified outcomes of the HGABCNN method

Images from two datasets are pre-processed using SMMF technique which is a combination of median filtering, morphological filtering, and edge-aware filtering to enhance breast images. Median filtering helps removing noise while preserving edges. Edge-preserving filter is used to retain tissue structures. Morphological filtering improves tissue structures by refining contours, which would further aid in segmentation and feature extraction. Input image is fed to median filter to remove noise, then morphological operations are performed to preserve tissue structure. For feature extraction, Pre-Self Swin Transformer is used. Its hierarchical structure captures fine details in tissue, temperature gradient in case of thermal image and then extract feature vectors. Histopathology and thermal images are resized and normalized before passing them to pretrained swin transformer model. Lastly self-adaptive correlation-constrained fuzzy C-means (SAC-FCM) clustering algorithm is applied. It is better than traditional FCM for segmentation as it detects nucleus and improves tumor segmentation. For thermal images it localizes the hotspots accurately by detecting temperature contrast regions. In the last step, for SAC-FCM Clustering, the image is normalized and flattened. The centroid positions and membership values are iteratively updated in the clustering process, where correlation

Table 2 Parameter settings of HGABCNN method

Parameters	Values for Proposed Method
Learning rate	0.001
Batch size	64
Iterations	100
Epochs	300
Optimizer	Gold rush optimizer

constraints help to boost the segmentation performance. After the algorithm has converged, the clusters are assigned to the most likely pixel, which produces a segmented image. The combination of these techniques aid in better quality of input images, feature extraction and segmentation of images used for BreakHis and thermal images. Table 3 displays the classified outcomes of the BC. In this table, the images from the two datasets are pre-processed, segmented and to get the classified result in detail shown in the Table 3.

4.3 Classified outcomes of the proposed method

Figures 2 and 3 showcases the training and testing loss and accuracy metrics specifically for the BreakHis and Kaggle dataset in a BC detection model. Initially, the model shows low accuracy in the early epochs due to random weight initialization. Around 50–100 epochs, accuracy increases significantly as the model learns hierarchical features. By 300 epochs, accuracy stabilizes near 98% benefiting from hyperbolic graph attention, which effectively captures complex spatial and texture patterns.

Initially the loss was high but starts decreases rapidly in the first 50 epochs as the model learns fundamental patterns. By 300 epochs, the loss reaches a near-minimal value indicating strong convergence. Loss is fluctuating slightly due to graph attention weights dynamically adjusting node relations in the hyperbolic space. Figure 2 and 3 depict accuracy and loss graph during training and validation. It exhibits accuracy and loss across 300 epochs for BC disease detection using BreakHis Dataset for histopathology images and Kaggle dataset for thermal images. Training metrics measure correctly predicted training examples, while validation metrics gauge properly predicted validation examples. Figure 4 shows the confusion matrix for (a) BreaKHis dataset of Histopathology images and (b) Kaggle dataset of thermal images.

4.4 Experimental outcomes of the proposed method

Assessing the HGABCNN model involved a comparison of key parameters like accuracy, F1-score, recall, specificity, and precision against several other models, including DTL [22], CNN-GRU [23], CNN-PS [24], CNN-RNN [25], CNN based CAD [26], DMR-IR [27], RANet-ADSVM [28], DEEP_Pachi [29], Ensemble model [30], SVM [31], BPBRW with ABO [32], TTCNN [35], IMPA-ResNet50 [36], M-FD [37], BCP-TL [38] and DML [39]. This comparison highlights the performance of the HGABCNN model in relation to these other models.

4.4.1 Comparison of BreaKHis dataset with current methods

Figures 5a–d shows the performances comparison using BreaKHis dataset for Histopathology images. The HGABCNN (Proposed) achieve the highest accuracy and precision, reaching 98.6%. CNN-PS and RANet also exhibit high accuracy around 95%, while CNN-RNN has a slightly lower accuracy at approximately 90%.

In terms of precision, RANet, DML and HGABCNN (Proposed) maintain the top performance with around above 98%, whereas CNN-PS and CNN-RNN show slightly lower precision. Regarding recall, RANet and HGABCNN (Proposed) again reach the highest value of above 98%, followed by CNN-PS and DML at around 95%, with CNN-RNN slightly lower at 90%. For F1-score, HGABCNN (Proposed) achieves the highest at above 98%, DML follows closely with 98%, and RANet, CNN-RNN and CNN-PS display

Table 3 Classified outcomes of the proposed technique

Data sets	Input images	Pre-processed images	Segmented images	Category	Classified outcomes
BreaK His dataset for Histopathology images	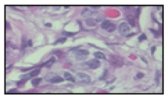	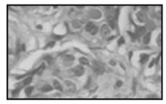	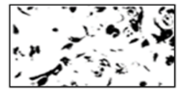	Benign tumors	Adenosis
	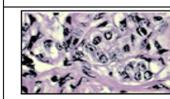				Fibroadenoma
	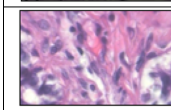	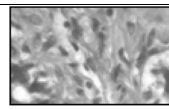	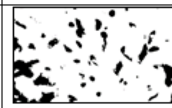		Tubular adenoma
	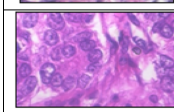	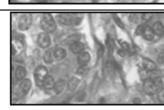	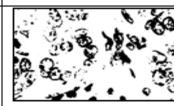		Phyllodes Tumor
	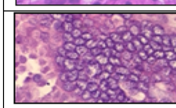		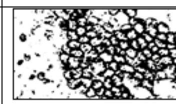	Malignant tumors	Ductal carcinoma
	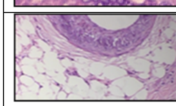	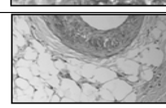			Lobular carcinoma
		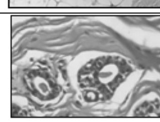			Mucinous carcinoma
	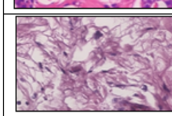	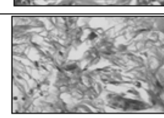	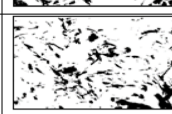		Papillary carcinoma
Kaggle dataset for	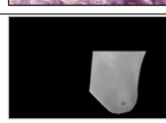	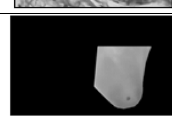	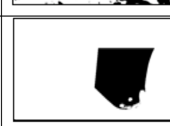	Normal	Healthy
thermal images	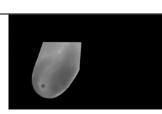	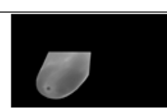		Abnormal	Unhealthy
			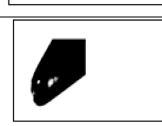		Unhealthy
	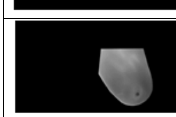	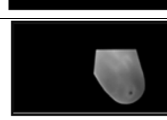			Unhealthy

scores ranging from 90 to 97%. Overall, the proposed HGABCNN method consistently demonstrates superior performance across all metrics.

4.4.2 Comparison of Kaggle dataset with existing methods

Figure 6 illustrates the evaluation of the (a) accuracy, (b) precision, (c) recall and (d) F1-score using the Kaggle dataset for thermal images. HGABCNN (Proposed) exhibited flawless performance, securing perfect scores across all metrics at 98%. Conversely, DMR-IR displayed lower scores with 86% accuracy, 84% precision, 90% recall

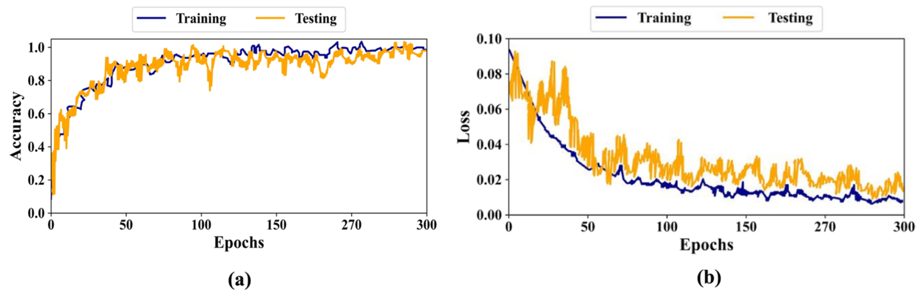

Fig. 2 Training and testing accuracy (**a**) and loss curves (**b**) of BreakHis dataset

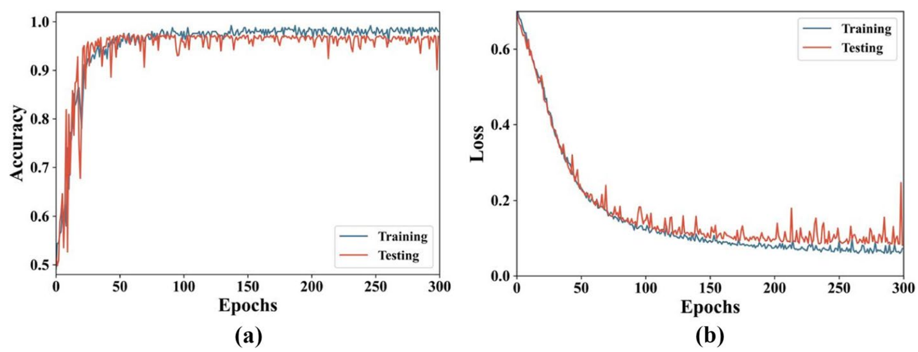

Fig. 3 Training and testing accuracy (**c**) and loss curves (**d**) of Kaggle dataset

and an F1-score of 87%. SVM excelled in precision (98.9%) but had slightly lower recall (90.47%), resulting in a 95% F1-score. VGG16 showed balanced performance with 97% across all metrics. These metrics collectively provide insights into each model's accuracy in predictions and positive case classification. Table 4 summarizes a comparative analysis of different BC recognition methods in terms of classification accuracy.

4.5 Ablation study

Ablation studies are essential for evaluating the contributions of various components in a deep learning model. For the BC detection system using HGABCNN, the ablation study involves systematically removing or altering components to observe their impact on performance.

The ablation study of the proposed method is illustrated in Table 5. The proposed model achieves performance metrics with 98.6% accuracy, 98.6% precision, 98% recall and 98.3 F1-score, demonstrating the effectiveness of combining all novel preprocessing and optimizing techniques. Accuracy is reduced significantly from 98.6 to 91.2% by considering only HGA and omitting BiCNN indicating its crucial role in capturing complex data relationships. Accuracy further drops to 89.3%, by including only BiCNN and excluding HGA highlighting its importance in feature extraction. The ablation study shows that model achieves 88.7% accuracy without HGA and 87.6% without BiCNN. The results clearly emphasize on the combined significance of these components for optimal performance. The absence of both HGA and BiCNN results in severe decrease in accuracy to 83.5%, showcasing the necessity of advanced graph attention and efficient data handling.

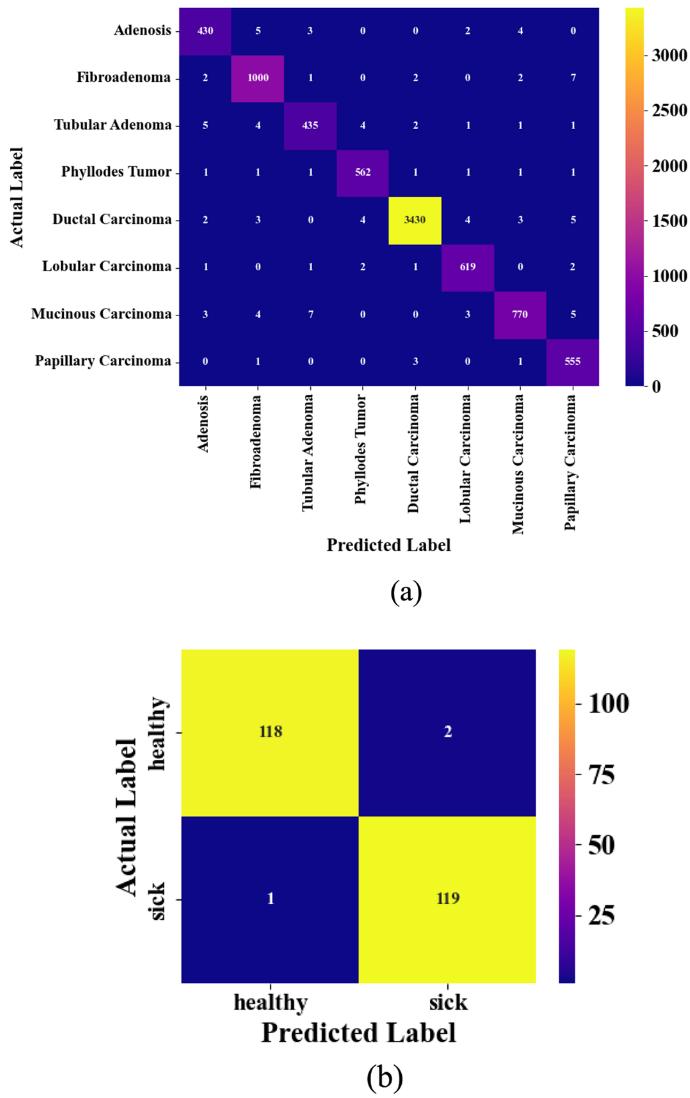

Fig. 4 Confusion matrix for (**a**) BreaKHis dataset for Histopathology images and (**b**) Kaggle dataset for thermal images

5 Conclusion and future scope

A novel method Hyperbolic Graph Attention with Bidirectional Convolutional Neural Network (HGABCNN) is introduced in this research to classify healthy and malignant breast. The integration of Adaptive Gold Rush Optimization technique has improved the performance of proposed method. The advanced prepossessing techniques such as Semantic edge-aware median morpho filtering to upgrade input image quality, Swin-based feature extraction technique to extract meaningful features from the refined images and self-adaptive correlation-constrained Fuzzy C-Means clustering segmentation technique are used in this research. The proposed method delivers exceptional outcomes, reaching peak accuracy of 98.6% along with high recall, F1-score, and precision, outshining other methods. This showcases its promise in advancing breast cancer detection and its potential for clinical application. The proposed method is a first step towards practical clinical use. Though it will be takes few years before it is incorporated

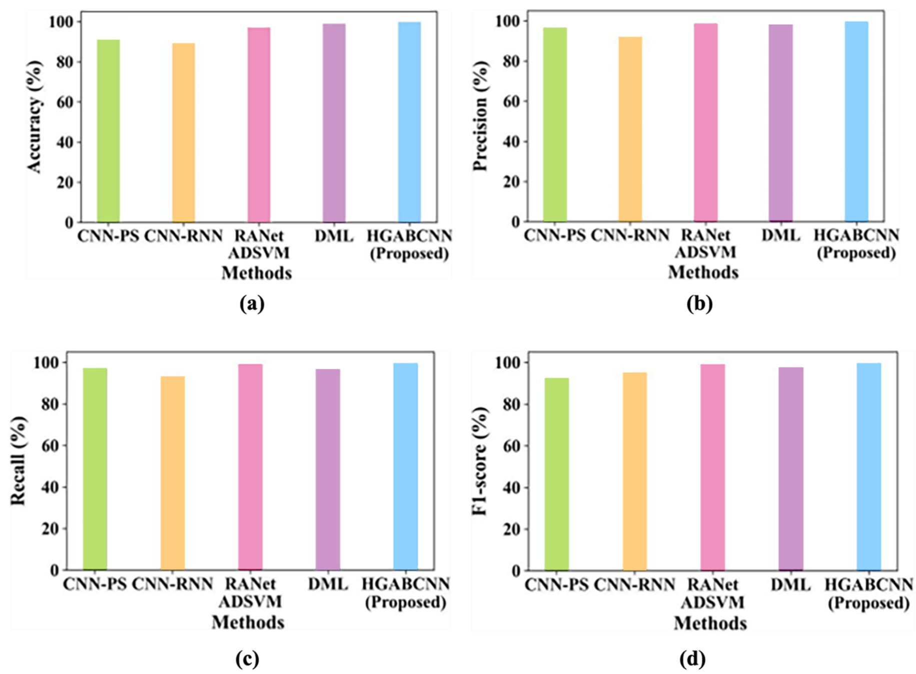

Fig. 5 **a** accuracy **b** precision **c** recall and **d** F1-score analysis using BreaKHis dataset

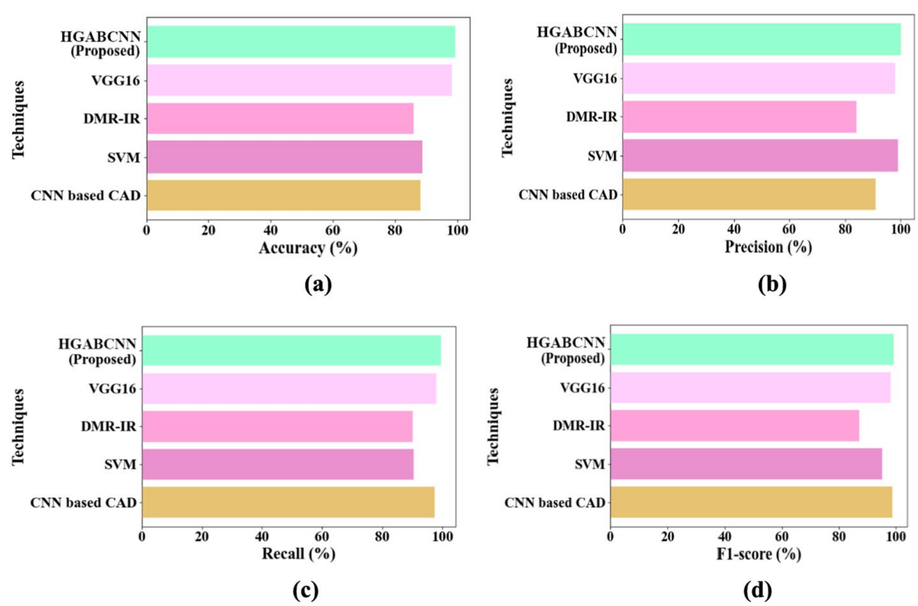

Fig. 6 (**a**) Accuracy (**b**) Precision (**c**) Recall and (**d**) F1 score analysis using Kaggle dataset

Table 4 Comparison of different BC recognition-based methods in terms of accuracy

BreakHis dataset		IR Thermal Images dataset	
Methods	**Accuracy (%)**	**Methods**	**Accuracy (%)**
CNN PS [15]	92.0	CNN based CAD [17]	87
CNN RNN [16]	90.5	SVM [20]	88
RANet ADSVM [19]	96.75	DMR-IR [18]	86
DTL [13]	97.06	VGG 16	97
HGABCNN (proposed)	98.6	HGABCNN (proposed)	98

Table 5 Ablation study of the proposed method

Experiment configuration	Accuracy (%)	Precision (%)	Recall (%)	F1-Score (%)
Full Model (HGABCNN)	98.6	98.6	98	98.3
With Hyperbolic Graph Attention (HGA)	91.2	89.5	92.0	90.7
With Bidirectional CNN (BiCNN)	89.3	88.0	90.1	89.0
Without HGA	88.7	89.2	89	88.6
Without BiCNN	87.6	87.1	87.9	87.5
Without HGA and BiCNN	83.5	82.2	84	83.1

into daily practice, it has great potential to improve the lives of pathologists, oncologists by automatic detection of BC and undoubtedly the field as a whole.

The proposed HGABCNN model demonstrates promising performance in breast cancer detection; however, few limitations need to be addressed. Due to the model's complexity, computational costs may go high, eventually limit real-time clinical deployment. Furthermore, while the integration of hyperbolic graph attention layers refines feature extraction, it may also amplify noise or irrelevant features in cases of poor-quality input images. The current work is limited to histopathology image and thermal image datasets, can be further expanded with other modalities such as mammography, MRI. Future work should focus on optimizing computational efficiency, incorporating adaptive hyperparameter tuning and implementing noise reduction techniques to improve robustness and practical applicability. This will be expanded further in the future by experimenting with bigger datasets, such as big data, real-time processing via edge computing.

Author contributions

S.P.: Conceptualization, methodology, data curation, writing—original draft preparation. V.B.: Writing—original draft, visualization, investigation, reviewing and editing, D. B.: Supervision, critical revision of the manuscript for intellectual content and editing, T.H.K.: Resources, investigation, formal analysis, critical revision of the manuscript.

Funding

No funding was received for conducting this study.

Availability of data and materials

All data generated and/or analysed during this study are available from the corresponding author on request. Further enquiries can be directed to the corresponding author. The datasets analyzed during the current study are publicly available: 1.BreakHis Histopathology Dataset (BreaKHis v1) – provided by the Visual and Industrial Computing Laboratory (VRI), Federal University of Paraná, Brazil. The dataset can be accessed at: http://www.inf.ufpr.br/vri/databases/BreaKHis_v1.tar.gz.. 2.Thermal Breast Cancer Image Dataset – provided by the Instituto de Computação, Universidade Federal Fluminense (UFF), Brazil. The dataset can be accessed at: http://visual.ic.uff.br/en/proeng/thiagoelias.

Declarations

Ethics approval

The paper is not currently being considered for publication elsewhere. This article does not contain any studies with human participants or animals performed by any of the authors. The dataset used is publicly available on Kaggle and contains anonymized data. Therefore, ethical approval was not required.

Consent to participate

This study did not involve human participants. Therefore, consent to participate was not required.

Consent for publication

All authors have reviewed the final version of the manuscript and consent to its publication in *Discover Oncology*. This research does not involve any individual person's data in any form (including individual details, images, or videos); therefore, no specific consent to publish is required.

Competing interests

The authors declare no competing interests.

Received: 19 February 2025 / Accepted: 11 September 2025

Published online: 25 November 2025

References

1. Chhichholiya Y, Ruthuparna M, Velagaleti H, Munshi A. Brain metastasis in breast cancer: focus on genes and signaling pathways involved, blood–brain barrier and treatment strategies. Clin Transl Oncol. 2023;25(5):1218–41.
2. Nikovia V, Chinis E, Gkantaifi A, Marketou M, Mazonakis M, Charalampakis N, et al. Current cardioprotective strategies for the prevention of radiation-induced cardiotoxicity in left-sided breast cancer patients. JPM. 2023;13(7):1038.
3. Zhang M, Mesurolle B, Theriault M, Meterissian S, Morris EA. Imaging of breast cancer–beyond the basics. Curr Probl Cancer. 2023;47(2):100967.
4. Khalid A, Mehmood A, Alabrah A, Alkhamees BF, Amin F, AlSalman H, et al. Breast cancer detection and prevention using machine learning. Diagnostics. 2023;13(19):3113.
5. Deng J, Liao X, Singh A, Singh A, Bhattacharya S. Research trends on AI in breast cancer diagnosis, and treatment over two decades. Discov Oncol. 2024;15(1):772. https://doi.org/10.1007/s12672-024-01671-0.PMID:39692996;PMCID:PMC11655727.
6. Tzeng YD, Hsiao JH, Chu PY, Tseng LM, Hou MF, Tsang YL, et al. The role of lsm1 in breast cancer: shaping metabolism and tumor-associated macrophage infiltration. Pharmacol Res. 2023;22:107008.
7. Restrepo JC, Dueñas D, Corredor Z, Liscano Y. Advances in genomic data and biomarkers: revolutionizing NSCLC diagnosis and treatment. Cancers. 2023;15(13):3474.
8. Mai HT, Ngo DQ, Nguyen HP, La DD. Fabrication of a reflective optical imaging device for early detection of breast cancer. Bioengineering. 2023;10(11):1272.
9. Silveira JA, da Silva AR, de Lima MZT. Harnessing artificial intelligence for predicting breast cancer recurrence: a systematic review of clinical and imaging data. Discov Oncol. 2025;16(1):135. https://doi.org/10.1007/s12672-025-01908-6.PMID:39921795;PMCID:PMC11807043.
10. Uchikov P, Khalid U, Dedaj-Salad GH, Ghale D, Rajadurai H, Kraeva M, et al. Artificial intelligence in breast cancer diagnosis and treatment: advances in imaging, pathology, and personalized care. Life (Basel). 2024;14(11):1451. https://doi.org/10.3390/life14111451.PMID:39598249;PMCID:PMC11595975.
11. Khan F, Amanullah SI, Selvarajan S. Linear regressive weighted Gaussian kernel liquid neural network for brain tumor disease prediction using time series data. Sci Rep. 2025;15:5912. https://doi.org/10.1038/s41598-025-89249-w.
12. Kumar A, Kumar M, Bhardwaj VP, et al. A novel skin cancer detection model using modified finch deep CNN classifier model. Sci Rep. 2024;14:11235. https://doi.org/10.1038/s41598-024-60954-2.
13. Muniyandi AP, Padmanandam K, Subbaraj K, et al. An intelligent emotion prediction system using improved sand cat optimization technique based on EEG signals. Sci Rep. 2025;15:8782. https://doi.org/10.1038/s41598-025-89904-2.
14. Maruthupandi J, Sivakumar S, Dhevi BL, et al. An intelligent attention based deep convoluted learning (IADCL) model for smart healthcare security. Sci Rep. 2025;15:1363. https://doi.org/10.1038/s41598-024-84691-8.
15. Fuladi S, et al. A reliable and privacy-preserved federated learning framework for real-time smoking prediction in healthcare. Front Comput Sci. 2025;6:1494174.
16. Kumari D, Naidu MVSS, Panda S, et al. Predicting breast cancer recurrence using deep learning. Discov Appl Sci. 2025;7:113. https://doi.org/10.1007/s42452-025-06512-5.
17. Dharani NP, GovardhiniImmadi I, Narayana MV. Enhanced deep learning model for diagnosing breast cancer using thermal images. Soft Comput. 2024;28:8423–34. https://doi.org/10.1007/s00500-024-09742-8.
18. Ibrahim TS, Saraya MS, Saleh AI, et al. Accurate breast cancer diagnosis strategy (BCDS) based on deep learning techniques. Neural Comput & Applic. 2025;37:4617–50. https://doi.org/10.1007/s00521-024-10849-0.
19. Ogundokun RO, Misra S, Douglas M, Damaševičius R, Maskeliūnas R. Medical internet-of-things based breast cancer diagnosis using hyperparameter-optimized neural networks. Future Internet. 2022;14(5):153.
20. Aldhyani TH, Khan MA, Almaiah MA, Alnazzawi N, Hwaitat AK, Elhag A, et al. A secure internet of medical things framework for breast cancer detection in sustainable smart cities. Electronics. 2023;12(4):858.
21. Lahoura V, Singh H, Aggarwal A, Sharma B, Mohammed MA, Damaševičius R, et al. Cloud computing-based framework for breast cancer diagnosis using extreme learning machine. Diagnostics. 2021;11(2):241.
22. Pati A, Parhi M, Pattanayak BK, Singh D, Singh V, Kadry S, et al. Breast cancer diagnosis based on IoT and deep transfer learning enabled by fog computing. Diagnostics. 2023;13(13):2191.
23. Wang X, Ahmad I, Javeed D, Zaidi SA, Alotaibi FM, Ghoneim ME, et al. Intelligent hybrid deep learning model for breast cancer detection. Electronics. 2022;11(17):2767.
24. Ahmad N, Asghar S, Gillani SA. Transfer learning-assisted multi-resolution breast cancer histopathological images classification. Vis Comput. 2022;38(8):2751–70.
25. Srikantamurthy MM, Rallabandi VS, Dudekula DB, Natarajan S, Park J. Classification of benign and malignant subtypes of breast cancer histopathology imaging using hybrid CNN-LSTM based transfer learning. BMC Med Imaging. 2023;23(1):19.
26. Yadav SS, Jadhav SM. Thermal infrared imaging-based breast cancer diagnosis using machine learning techniques. Multimedia Tools Appl. 2022;1:1–9.
27. Alshehri A, AlSaeed D. Breast Cancer detection in thermography using convolutional Neural Networks (CNNs) with deep attention mechanisms. Appl Sci. 2022;12(24):12922.
28. Zhou Y, Zhang C, Gao S. Breast cancer classification from histopathological images using resolution adaptive network. IEEE Access. 2022;31(10):35977–91.
29. Tippannavar SS, Gayathri S, Swetha S. Breast Cancer Detection and Classification using Random Forest and KNN on Kaggle Breast Cancer Data using Mammography.
30. Dewangan KK, Dewangan DK, Sahu SP, Janghel R. Breast cancer diagnosis in an early stage using novel deep learning with hybrid optimization technique. Multimedia Tools Appl. 2022;81(10):13935–60.
31. Pradhan K, Patra S. Semantic-aware structure-preserving median morpho-filtering. Vis Comput. 2024;40(2):505–21.
32. Wang Y, Wang H, Lu W, Yan Y. HyGGE: hyperbolic graph attention network for reasoning over knowledge graphs. Inf Sci. 2023;1(630):190–205.
33. Gao J, Yang D, Wang S, Li Z, Wang L, Wang K. State of health estimation of lithium-ion batteries based on Mixers-bidirectional temporal convolutional neural network. J Energy Storage. 2023;20(73):109248.
34. Sarjamei S, Massoudi MS, Esfandi SM. Gold rush optimization algorithm. Iran Univ Sci Technol. 2021;10(11):291–327.
35. Maqsood S, Damaševičius R, Maskeliūnas R. TTCNN: a breast cancer detection and classification towards computer-aided diagnosis using digital mammography in early stages. Appl Sci. 2022;12(7):3273.

36. Houssein EH, Emam MM, Ali AA. An optimized deep learning architecture for breast cancer diagnosis based on improved marine predators algorithm. Neural Comput Appl. 2022;34(20):18015–33.
37. Zebari DA, Ibrahim DA, Zeebaree DQ, Mohammed MA, Haron H, Zebari NA, et al. Breast cancer detection using mammogram images with improved multi-fractal dimension approach and feature fusion. Appl Sci. 2021;11(24):12122.
38. Diwakaran M, Surendran D. Breast cancer prognosis based on transfer learning techniques in deep neural networks. Info Technol Control. 2023;52(2):381–96.
39. Kaur A, Kaushal C, Sandhu JK, Damaševičius R, Thakur N. Histopathological image diagnosis for breast cancer diagnosis based on deep mutual learning. Diagnostics. 2023;14(1):95.
40. BreakHis Histopathology dataset: http://www.inf.ufpr.br/vri/databases/BreaKHis_v1.tar.gz
41. Thermal image dataset: http://visual.ic.uff.br/en/proeng/thiagoelias

Publisher's Note